Optically Feeding 1.75 W With 100 m MMF in Efficient C-RAN Front-Hauls With Sleep Modes

Juan Dayron López Cardona, Pedro Contreras Lallana, Ruben Altuna, Alicia Fresno-Hernández, Xabier Barreiro, and Carmen Vázquez, *Senior Member, IEEE*

***Abstract*—Using bundles of multimode optical fibers (MMF) as part of the 5G centralized radio access networks front-haul solutions for optically powering of low power consumption Remote Radio Heads (RRH) is proposed and experimentally demonstrated with 100 m of 200 μm core diameter MMF. From the 34.85 W electrical power provided to the system, 1.748 W are delivered to the load, giving an overall 5% efficiency, being the temperature controller of the High Power Lasers the most critical element. If intermediates results are considered, the efficiency from input optical power to electrical power after the PV cells is 43.4%. The RRH manages 2.34 W for control, battery charge, communications and the load operation. The system includes a low power bidirectional control channel that provides the capability of enabling different sleep modes and sending information about the status of the battery and sensing elements at RRH. The RRH has a minimum power consumption of 3.15 mW. Optimized design of different elements of the system are included. The system is tested by feeding a RF power amplifier at the RRH; providing a stable power supply and EVM performance below 17.8% with QPSK on a 20 GHz RF carrier.**

***Index Terms*—5G signals, multimode fiber (MMF), power over fiber (PoF), radio access networks (RAN), radio over fiber (RoF), remote radio heads (RHH), sleep modes.**

I. Introduction

POWER over fiber (PoF) is a good strategy for providing energy to remote points free of electromagnetic interference, with low weight, good galvanic isolation and with an easy integration in the infrastructure of telecommunication operators. This technology can be used in different applications such as optically powered medical devices [1], optically powered sensors [2]–[4], passive optical networks (PON) monitorization [5]–[6], or optically powered fiber networks [7]–[9], among others.

Optical fibers are also one of the supporting technologies for the increasing capacity of 5G radio access networks (RAN), as part of the back/front haul infrastructure for transmitting radio–over-fiber (RoF) signals. Higher data rates for RF signals implies the reduction of the remote radio heads (RRH) coverage, increasing the number of RRHs deployed. Therefore, it is important to reduce their power consumption as well as costs of installation, operation and maintenance. In this way, PoF can simultaneously transmit optical data and power in the optical fiber. It can provide the power required by the RRH from the central office (CO), and centralize the power source in the CO in order to share costs in a C-RAN scenario using the PoF pooling concept described in [10]. PoF is proposed as a technology to optically power RRHs and/or Remote Antenna Units (RAU) [11]–[15]. In addition to this, sleep mode strategies to reduce power consumption in C-RAN are proposed to improve the system efficiency and performance [16], [17]. Some densification analysis show that if the Base Stations (BS) density increased from 1BS/km^2 to 100 BS/km^2 the average transmission link length is reduced 10-fold from 500 m to 50 m [18]. The high connectivity demand on emerging 5G fields includes cases compatible with the use of PoF in 100 m links [19].

State of the art of mostly partial optical powering of RRHs, proposes the use of different types of optical fibers according to the different scenarios. Standard single mode fibers (SMF) that make use of the existing infrastructure are limited to input powers of several Watts. Multimode fibers (MMF), multicore fibers (MCF) or double cladding fibers (DCF) are also studied for delivering the energy. First experiments with 200 μm core diameter MMFs provided efficiencies (the ratio of input optical power to electrical power after photovoltaic conversion) of 50% at 12 m [20], that were reduced to 5% at 300 m and 50 μm core diameter MMF [21]. Afterwards, using DCF [22] as the transmission media, they reached 10% efficiency at 100 m, launching an optical power of 4 W at 830 nm and providing 400 mW in the remote nodes. Meanwhile in [23], a 28.6% efficiency is reported with 43 W of electrical power delivered to the load at 300 m by injecting an optical power of 150 W. In this last case, the DCF is equivalent in size to 18 MMFs of 105 μm core diameter each. An intermediate transition to 6 MMFs is used to reduce the insertion losses and improve the overall efficiency.

A summary about the main achievements in PoF applied to RoF is reported in [24]. Some propose the integration of PoF and RoF with multicore fibers as a solution in the large scale of small cell systems suggested for 5G [12] and using PoF to reduce the number of power supplies. Others [23] point out the need of

Manuscript received January 20, 2021; revised April 8, 2021; accepted May 6, 2021. Date of publication May 11, 2021; date of current version December 16, 2021. This work was supported in part by the Spanish Ministerio de Ciencia, Innovación y Universidades, Madrid Government (Comunidad de Madrid-Spain) and H2020 European Union programme under Grants RTI2018-094669-B-C32 and Y2018/EMT-4892, in part by Multiannual Agreement with UC3M in the line of Excellence of University Professors under Grant EPUC3M26, and in part by the context of the V PRICIT (Regional Programme of Research and Technological Innovation) and 5G PPP Bluespace project under Grant n°.762055, respectively. *(Corresponding author: Carmen Vázquez.)*

The authors are with Electronics Technology Department, Universidad Carlos III de Madrid, Leganés, 28911 Madrid, Spain (e-mail: julopezc@ing.uc3m.es; pcontrer@ing.uc3m.es; raltuna@pa.uc3m.es; afresno@ing.uc3m.es; xbarrero@pa.uc3m.es; cvazquez@ing.uc3m.es).

Color versions of one or more figures in this article are available at https://doi.org/10.1109/JLT.2021.3078848.

Digital Object Identifier 10.1109/JLT.2021.3078848

simple and cost effective installations of RAUs, considering the cost of installing electrical equipment and wiring from nearby power lines in addition to installing communication equipment; apart from minimizing the impact of power outages by using PoF. 5G technology is up to 90% more efficient per unit of traffic than previous wireless technologies, but more actions are needed to improve efficiency and minimize CO_2 emissions [25]. PoF provides remote control to improve efficiency using sleep modes in idle periods independently of power grid, giving an advantage to operators. In the urban areas with dense cell deployment, where the power grid is available, this technology can provide a minimum energy in an independent way allowing connectivity and recording images in areas requiring a special security, even in the case of a blackout. PoF can provide better coverage in a specific area, directly controlled by the operator, allowing a different quality of service at a different cost. This technology provides a direct control of the infrastructure. PoF aim is not to replace or substitute all the mobile front-haul topology traditional power sources. In rural areas, some specific critical infrastructures need a good coverage and special protection against natural disasters where PoF can provide an additional back up system in case of failure.

In this paper, we propose a 100 m PoF system capable of delivering 1.748 W to a load that can reduce the overall power consumption by controlling and using different sleep mode configurations in an ARoF fronthaul scenario where it is experimentally tested. Firstly, section II describes the system configuration integrated in C-RAN architecture and the main elements. In Section III, the design of the building blocks of the system is presented. Section IV includes the experimental setup for evaluating the performance of the power delivery in 100 m MMF link with communications, control and power consumption disaggregation. We also evaluate the different functionalities and the stable feeding of a power amplifier in an ARoF link with QPSK on a 20 GHz RF carrier. Finally, Section V concludes the paper.

II. System Configuration

The system, where the PoF module is integrated, consists of a central office (CO) located in the Base Band Units (BBU) pool area of the C-RAN, see Fig. 1a, a remote receiver unit as part of a RRH and a bidirectional communication between them. We add a PoF layer to the ARoF fronthaul described in [26] based on bundles of MMF for powering. PoF system can feed low power 5G RRHs or some parts of them. It can also control the feeding of specific parts or making them enter into sleep mode operation, for example switching off the power amplifiers (PA). The CO has different High Power Lasers (HPL), a communication (COM) unit and a control unit, as shown in Fig. 1b. The RRH has an energy management unit with the Photovoltaic cells (PV), different regulators (LDO and DC/DC), control and communication units. In the optical plane, downlink/uplink communication at 1310 nm uses dedicated SMFs (see Fig. 1b), while PoF delivery uses a bundle of 200 μm diameter MMFs. Those MMF fibers can also replace the SMFs used in communications. An overview of the PoF system specifications is given in Table I.

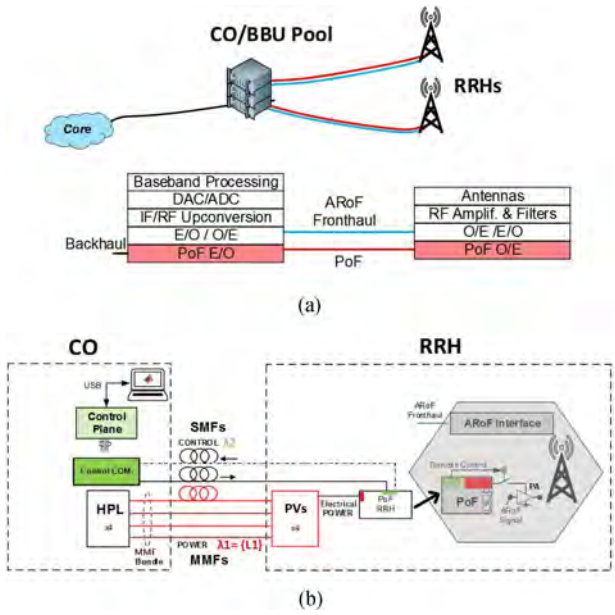

Fig. 1. Schematic of the PoF system: (a) Within C-RAN, (b) Main elements. CO: Central office. BBU: Base band unit. RRH: Remote radio head. ARoF: Analog radio over fiber. PoF: Power over fiber. HPLs: High power lasers. PVs: Photovoltaic cells. COM: Communications. PA: Power amplifier.

TABLE I
MMF-PoF System Specifications

Optical fiber feeding	Bundle of 100 m 200 μm diameter MMFs
Fiber Loss	3dB/km
HPL	Set of 808 nm 1.5 W lasers
PV cells	45.8% optical to electrical efficiency
RRH output voltage	5 V
RRH feeding power	1.748 W(electrical)
RRH sleep mode 1A	257.58 mW (electrical)
RRH sleep mode 1B	150.94 mW (electrical)
RRH sleep mode 2	3.15 mW (electrical)

III. Building Blocks Design

The different elements included at CO and RRH are shown in Fig. 2, with the building blocks described next.

A. Central Office (CO)

The 808 nm HPLs are at the CO (see left side of Fig 2). The controlled and/or monitored RRH parameters by the CO are:

-input current sensor (CS) proportional to input power,
-sensing parameters (temperature and humidity),
-percentage of charging battery,
-battery status (charging/discharging)
-control of PoF energy management unit for powering the load or charging the battery,
-configuration of two sleep mode scenarios (enter or awake) with different functionalities:

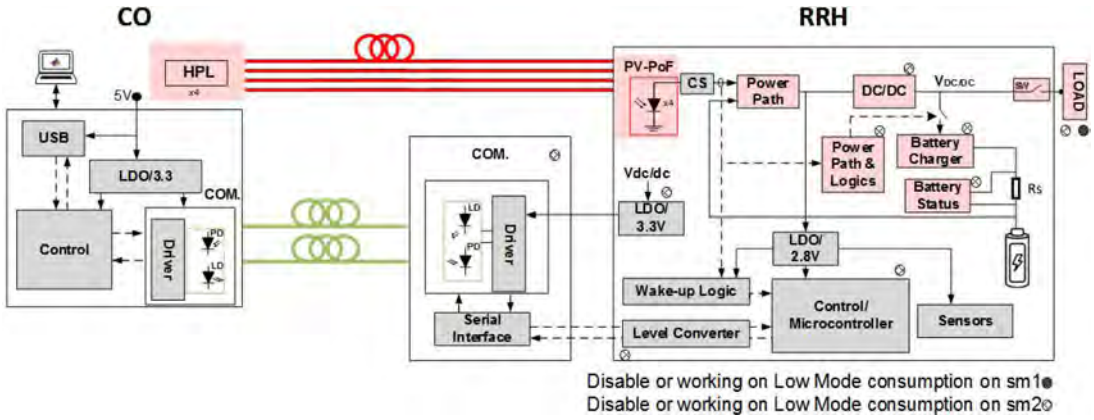

Fig. 2. Schematic of different building blocks of the MMF-PoF system: Main and communications boards at CO and RRH side, including elements supporting sleep mode operation: •sm1, ○sm2. LDO, and DC/DC regulators. CS: Current sensors.

Fig. 3. Photograph of PCB at CO and HPLs controlled.

- sleep mode 1 (sm1): load is disconnected but RRH is listening (A: battery charging connected, B: battery charging disconnected)
- sleep mode 2 (sm2): minimum power consumption, the communication channel is also disconnected. It can be awaken by hardware with monitoring parameters saved in the microcontroller memory.

Apart from controlling the RRH, the CO provides the optical power delivery and switching control capabilities to activate the different HPLs.

B. Remote Receiver Unit as Part of RRH

The RRH hardware consists of two boards (Main and Communication board) controlled by a MSP430 microcontroller. The Main board includes the GaAs PV cells that can power the load and the control system.

During the operation, the PV cells heat up by dissipated power. A specific heatsink to prevent PV cells from overheating is designed using *Solidworks* software. Simulations include six PV cells with a maximum input optical power of 2.5W per cell and an efficiency of 45.8%. The material used is aluminum with 135W/(m·°C) thermal conductivity and 10W/(m^2·K) convection. We have considered an unfavorable scenario where the PV cells dissipate the heat only through its bottom side in contact with the aluminum heatsink and in two configurations: placing them linearly or forming a circle in a disk. According to the simulations (see Fig. 4), the disk dissipates the heat at least three times better.

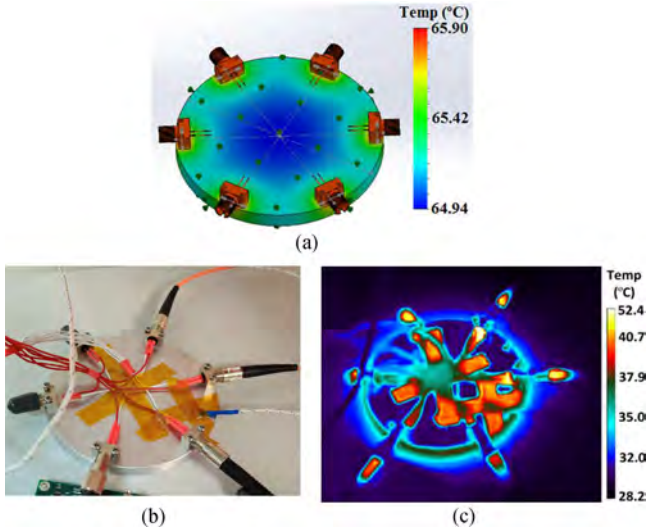

Fig. 4. (a) Simulations of power dissipation at PV cells considering each PV cell receives 2.5W optical power. (b) Photograph of PV cells within the heatsink. (c) Thermal image of the heatsink after eight minutes working with four PV cells receiving a total input optical power of 5.12 W.

We simulate the behavior of four disks with diameters of 10, 20, 30 and 50 mm. The PV cells temperature decreases from 108 °C to 66 °C when the diameter increases up to 50 mm. Fig. 4(a) shows the simulation of the 50 mm aluminum disk. Fig. 4(b) shows a picture of the PV cells placed in the heatsink. Fig. 4(c) is the thermal image after eight minutes working with only four PV cells illuminated with a total input optical power of 5.12 W. The maximum temperature for this situation is less than 40 °C, far from the 66 °C obtained in the simulations where the total input optical power considered is 15 W.

C. PoF Feeding MMF Fiber

The maximum power that an optical fiber handle depends on the effective area of the first order mode that is proportional

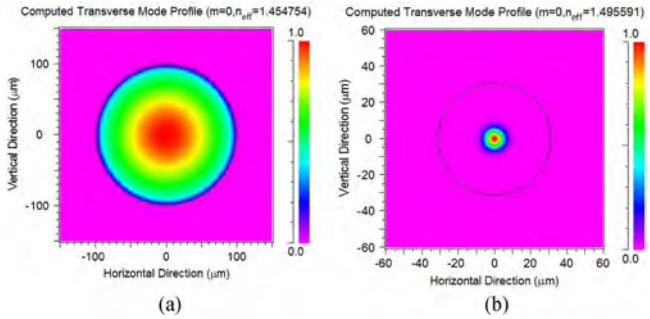

Fig. 5. (a) Simulation of the MFD of a 200 μm core MMF. (b) Simulation of the MFD of an OM1 MMF.

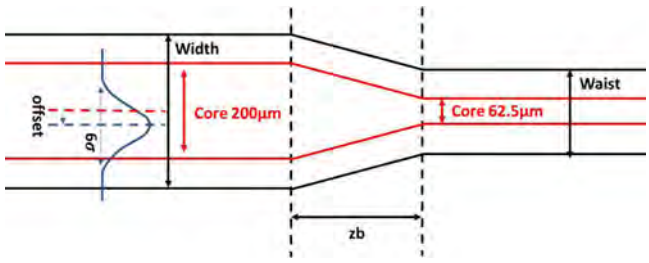

Fig. 6. Cross section of a MMF taper from a core diameter of 200 μm to 62.5 μm, the width of the input field is 6σ and it is launched with a displacement respect to the fiber center (offset).

to its Mode Field Diameter (MFD) [27]. Fig. 5(a) and (b) show simulations with *RSoft* software to determine the MFD of different commercial MMFs with a core diameter of 200 μm (step-index-SI) and 62.5 μm (graded-index-GI) respectively. Considering the threshold power density of silica optical fibers is around 2.5 MW/cm^2, the maximum allowable optical power is 639 W for the SI 200 μm MMF and 2.1 W for the GI 62.5 μm MMF; apart from the practical connector limitations.

The attenuation of the two optical fibers is around 3 dB/km and 2.5 dB/km for the 200 μm and 62.5 μm respectively, both at 808 nm. The 200 μm MMF is more expensive. On contrast, the GI 62.5 μm OM1 fiber is a standard fiber deployed and there are other compatible passive components available.

Anyway, 200 μm MMFs are used in our setup because they have an optimum coupling efficiency with the HPLs and transmit high optical powers without damage. Future approaches can consider hybrid solutions by using the 200 μm diameter MMF in the first meters of the link, where there is more power, and changing to the commercial OM1 fiber afterwards. One possible solution for passing from one fiber to the other is by means of a tapper as shown next.

D. MMF Taper From 200 μm to 62.5 μm Core Diameter

To achieve a lower cost and good power efficiency we propose coupling the HPL to a SI 200 μm diameter MMF and then, use a taper from 200 μm MMF to a more conventional 62.5 μm diameter MMF, as shown in Fig. 6. The purpose of this section is to theoretically analyze the feasibility of the proposal by checking if it can meet the efficiency commitments of our system.

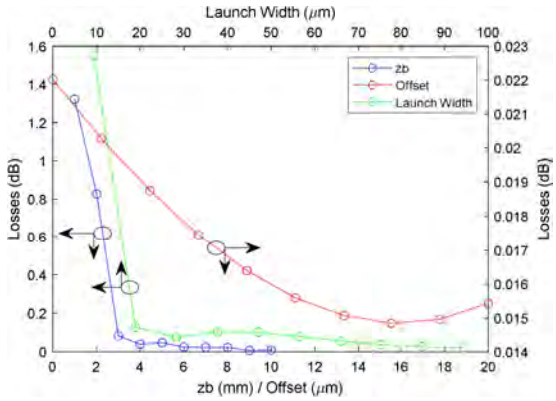

Fig. 7. Left y-axis and bottom x-axis: Losses as a function of length values of the drop zone of the taper (z_b). Left y-axis and top x-axis: Losses as a function of the width of the launch field. Right y-axis and bottom x-axis: Losses as a function of the offset of the launch field.

We use a gaussian launch field at an 808 nm wavelength with $6\sigma = 200$ μm, so the 1/e width is 94.26 μm. In the simulations, we take into account that the initial 200 μm MMF has a numerical aperture NA $= 0.22$ and a SI profile, while the final 62.5 μm fiber has a NA $= 0.275$ and a GI profile. Using the Sellmeier equation for the given wavelength, the refractive index of the cladding is $n_2 = 1.453$. The refractive indexes of the core, n_1, for each fiber is calculated using the NA.

The designed taper has a core width of 200 μm, and a waist width of 62.5 μm, being the waist width the one corresponding to the thinner section (see Fig. 6). The drop zone of the taper (z_b) is 7 mm long, and the straight zone after the drop zone is another 7 mm long. With these conditions and using *RSoft* software, the result for the losses is $L = 0.022$ dB, so, the simulated taper should allow to maintain the commitment to efficiency. To reinforce the obtained results, the main parameters that can affect the taper losses are analyzed.

The three parameters taken into account are the width of the input field, the offset and the length of the drop section, z_b. The taper losses in dB, when modifying the different variables, are shown in Fig. 7.

An optimal offset value minimizes the losses. The longer z_b and wider the input field, the smaller the losses. We check that the losses of the taper are small enough, and therefore it can be part of our future PoF system.

IV. Experimental Set-Up and Measurements

In 5G C-RAN deployments, PoF power can be sent in a dedicated fiber or can share the fiber by wavelength division multiplexing with the RoF signal, being called dedicated or shared scenarios [24], [28]. In our experiments, we focus on providing the highest power with a good efficiency at the RRH, so a dedicated scenario is initially tested. In Fig. 8, there is a schematic and a photograph of the experimental set-up.

A. Lasers System Analysis

The design of the laser system is energy efficiency driven. The use of 808 nm semiconductor lasers as HPLs coupled to

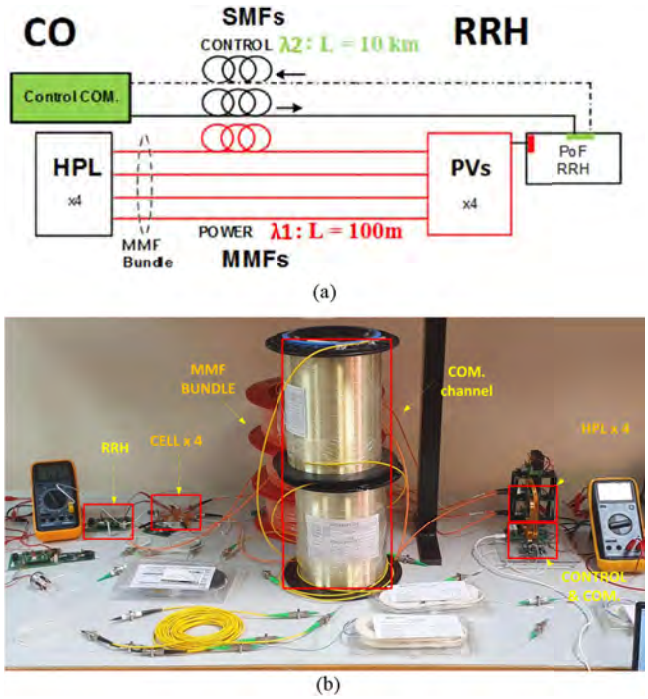

Fig. 8. Experimental setup: (a) Schematic. (b) Photograph.

TABLE II
EXPERIMENTAL SET-UP POWER BALANCE DATA

All 4 808 nm HPLs power	5.405 W
Total optical fiber loss	0.285 W
All 4 PV cells received power	5.12 W

200 μm MMF fibers minimize the coupling losses. From the total electrical power provided to the HPLs, 34.85 W, the emitted optical power is 5.407 W, then, the efficiency of the laser system is 15.7%. The design includes a temperature controller (TEC) with a Peltier and heatsinks for the proper operation of the system. The cooling system consumes 17.77 W that is more than half of the input power. The electronics allow to control the laser operation and switching on and off each module if required.

B. Optical Power Budget Analysis

The optical power delivery system uses spools of 200 μm core diameter MMFs for the PoF and two spools of G652.D SMF, for uplink/downlink communications (see Fig. 8). The length of the communication link is defined by other experiments, but can be reduced if required.

Each MMF connects a HPL with a GaAs PV cell. The optical power received in each PV cell of the RRH is the power supplied by the HPL in dBm, minus the losses of the optical fiber in dB. The typical attenuation coefficient in the data sheet of our 200 μm diameter MMF is 3 dB/km at 808 nm, thus, there is a maximum theoretical power loss of 0.3 dB in every 100 m MMF link. A summary of the losses of the PoF optical link are shown in Table II.

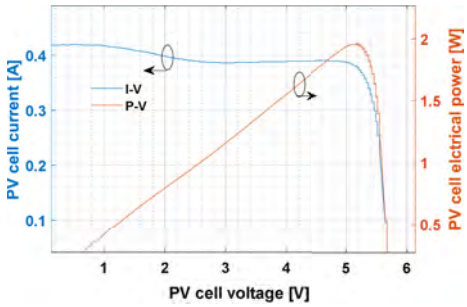

Fig. 9. Measurements of P-I and I-V curves of the PV cells.

C. Photovoltaic Cell and DC/DC Characterization

Fig. 9 shows the measured P-V and I-V curves of the group of 4 PV cells for an overall input optical power of 5.12 W. The maximum power point (MPP) is at a voltage around 5 V and 0.393 A output current. The conversion efficiency is around 45.8% with no overheating of the PV cells thanks to the designed heatsink shown in Fig. 4.

Considering that the maximum electrical power delivered to the load is 1.748 W, the measured efficiency of the DC/DC converter with a Maximum Power Point Tracking (MPPT) is 75.3%.

D. Power Consumption Analysis and Sleep Mode Operation

The scenarios analyzed in terms of power consumption at the RRH are scenarios for feeding a full low power RRH (some commercial systems promise consumptions of 5G nodes below 1 W) or some of the RRH components as the Power Amplifiers (PA), or the RRH in sleep mode. The inclusion of the battery can provide an extra power for feeding these components in short periods of time.

There are two different sleep modes. In sleep mode 1, the load is disconnected but the RRH is listening through the communication channel with two possible configurations consuming 257.58 mW if the battery is charging or 150.94 mW when it is not charging. Meanwhile, the minimum consumption obtained is 3.15 mW in sleep mode 2. In this mode, the RRH keeps saving the monitoring parameters that will be sent to the CO when the communication channel is awaken. Sankey diagram of the full system from electrical input power to electrical output power is shown in Fig 10.

As it is mentioned in section IV-A, from the 34.85 W electrical power provided to the system, 1.748 W are delivered to the load. In the CO, more than half of the power is used for cooling the laser; from the point of view of the PoF optical link power budget (transmission) and remote receiver unit (RRH) power budget. The losses of the 100 m MMF bundle are 0.285 W and the optical power received at the RRH side is 5.12 W. The efficiency of the optical to electrical conversion is 45.8%, providing 2.343 W of electrical power for the RRH components. Then, the efficiency from optical power launched at the CO to electrical power after the PVs cells, as usually reported [23], is around 43.4%.

The control system only consumes 16.47 mW, providing 1.748 W to the load. Taking into account this diagram, the overall

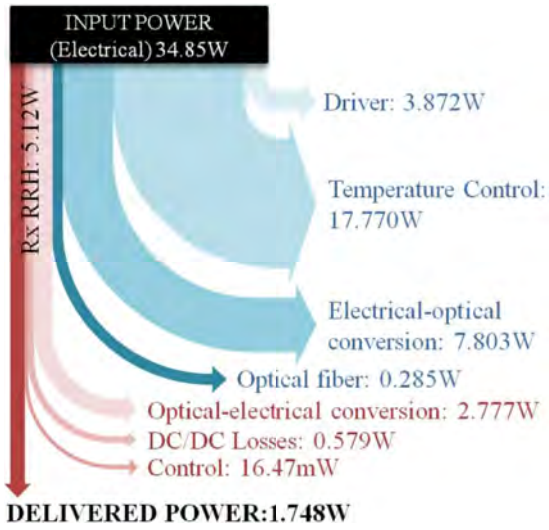

Fig. 10. Sankey diagram of the 100m optical PoF power link. Starting with the input electrical power, HPL driver, TEC, conversion efficiency, PoF optical link power budget including transmission, opto-electrical conversion, energy management and control electronics. Data shown for 1.748 W delivered power at output voltage of 5 V with 6.6 kbits/s bidirectional data transmission.

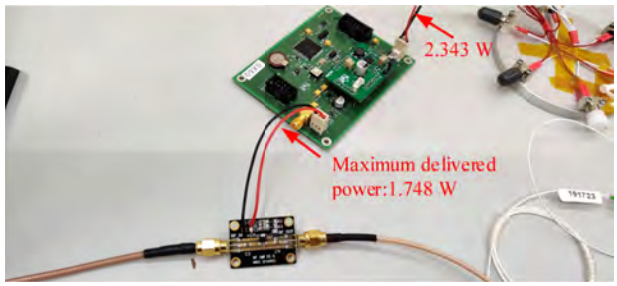

Fig. 11. PV cells feeding a RF-PA at the RRH, where 2.343 W is the electrical power delivered by the photovoltaic cells and a maximum of 1.748W can be supplied to the load.

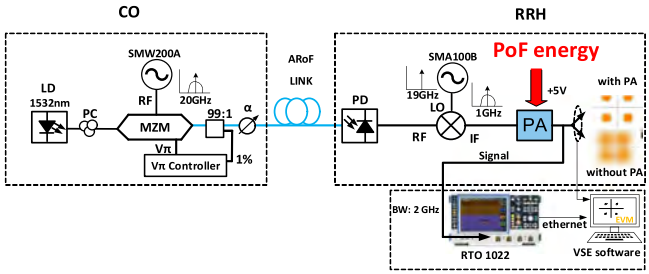

Fig. 12. Schematic of ARoF transmission over SMF, with intermediate frequency PA fed by PoF to increase the SNR and improving the EVM.

efficiency of the system, considered as the electrical power delivered to the load divided by the electrical power provided to the lasers, is 5%.

If we only consider the efficiency from optical power emitted by the HPLs, the efficiency rises to 32.3% including all the intelligence performed at the RRH. In all cases, RRH operates at 4 MHz. A small amount of the 1.748 W power delivered to the load is used for feeding the communications board and the battery charging. The communications board requires 33 mW, and the battery is charged with 20 mA at 4.2 V and it can provide extra 100 mW to the load when required. In the case of the RRH entering in any of the sleep modes, there is a reduction of more than 3 W in the power consumption at the remote site.

E. Functionality Tests and Discussion

In order to check the system functionality, different basic tests are defined and implemented using an application developed in *Matlab*. Those tests include displaying parameters at CO such as battery status or sensing parameters; the control from the CO (software/hardware) to make the RRH going in and out of both sleep modes. In addition, as a proof of concept, the proposed PoF system is used for feeding the Radio Frequency Power Amplifier (PA) at the RRH in an ARoF transmission over SMF, see a photograph of the connection in Fig. 11. The set up includes a LD operating at 1532nm, a polarization controller (PC), a vector generator (SMW200A) capable of generating frames that comply with 5G numerology, a MZM modulator, a MZM polarization controller, and a variable attenuator configured to a fixed attenuation (α), see Fig. 12. The generator is configured to generate Test Model 1.1 (TM1.1), with a 5 MHz bandwidth, QPSK modulation, a 20 GHz RF carrier and using Frequency Division Duplex (FDD), which is one of the two transmission modes used by the standard. On the receiving side, there is a mixer and an external generator configured at a working frequency of 19 GHz to generate an intermediate frequency of 1 GHz. The generation of this intermediate frequency is necessary because the acquisition is performed using an oscilloscope with a maximum bandwidth of 2 GHz, meanwhile the demodulation and analysis is performed using the R&SVSE software from a PC. Both elements are connected via a Cat5e Ethernet cable, enabling remote analysis. This configuration is a standard R&S solution used for this purpose.

In this scenario, the EVM measured was 55%, which did not meet the standard. We add an intermediate frequency PA with a gain of 20 dB at 1 GHz, to increase the SNR to improve the EVM. The amplifier has an electrical power consumption of 380 mW (76 mA @ 5 V) providing -55 dBm output power. Meaning that the amplifier can be remotely fed by the PoF system. Cascading amplifiers optically powered, as the PoF system delivers up to 1.748 W, can increase the output power. We check that the supply voltage is stable enough not to deteriorate the EVM. We verify both the stability of the voltage supplied by the PoF system and the stability of the EVM, being the PA fed by the PoF system for 60 minutes.

We use a 50 Ω resistor to measure the stability of the output voltage, as a replacement for the PA in terms of power consumption. This resistor corresponds to a consumption of 500 mW that is slightly higher than that of the amplifier, being a more restrictive condition in terms of evaluation of the output noise and power to be supplied by the PoF system. The measured noise is lower than 50 $\mathrm{mV_{rms}}$. On the other hand, the stability of the EVM is checked by successive measurements taken every 2 minutes and the results are shown in Fig. 13. The EVM fluctuations are mainly due to the drift of the MZM modulator. These variations are partially reduced by using a modulator bias controller. The measurements shown in Fig. 13 are for

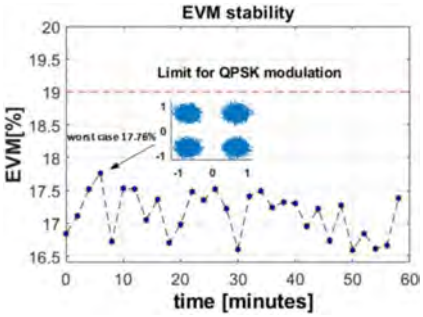

Fig. 13. EVM stability of the ARoF transmission system, with $\alpha = 8$ dB. Measurements every 2 minutes, the EVM fulfills the standards in the case of a QPSK modulation.

$\alpha = 8$ dB, which is selected as the worst-case scenario. The EVM remains below 17.8% that fulfills the standard limit for QPSK modulation. In the experiments, the EVM value greatly improves from 55% to less than 18%. The best EVM value obtained in the experiment is 2.93%, for $\alpha = 0$ dB.

Now, we compare the system proposed in this work with the one described in [23]. The efficiency, considering only the optical to electrical conversion (there is no information about the electrical power supplied to the LDs) is approximately 28.7%, while in our systems is near 32.3%. Taking into account that the optical fiber input power is 5.405 W and we deliver 1.748 W to the load. This efficiency increases up to 43.4% considering only the electrical power at the output of the PV cells as in [23], without the intelligence at RRH.

On the other hand, there is a system that delivers 5.5 W to the load with data transmission multiplexed over a 1.5 m of 400 μm core diameter MMF [29]. This system has an overall efficiency of 11.2% and provides feedback control for adapting the LD optical power to the load requirements.

Despite the lower overall efficiency, our system delivers power at 100 m, can charge a battery and has sleep mode operation for reducing the power consumption and the overall system efficiency. Comparing both Sankey diagrams the main difference between the efficiencies of both systems is related to the laser cooling, while their system uses 10.2 W, we require 17.7 W in the TEC. We have designed the transmitter in a compact way using a FC/PC metallic connector, and the cooling system is based on a Peltier cooler attached to the LD for reducing the cooler size. Our DC/DC implementation ensures the stability of the electrical power delivered to the load. By improving the efficiencies of the TEC, the electrical-optical conversion and the optical-electrical conversion to their values, the overall efficiency of our system could rise up to 11.3% with our additional capabilities. Increasing the heatsink size and placing the HPLs far away, if CO has no footprint limit, can help.

V. Conclusion

In this paper, we successfully demonstrated a PoF system based on 100 m length 200 μm core diameter MMF capable of delivering 1.748 W to a load. The overall efficiency of the system is 5%, but if we consider intermediate results, the efficiency from input optical power to electrical power after the PV cells is 43.4%, providing 2.34 W of electrical power to the RRH. The RRH includes batteries that can be used for feeding the load. A bidirectional control channel is included in the CO and the RRH, thus providing information about the status of the battery and sensing elements at RRH. The power consumption of the control unit is below 33 mW. In addition to this, the RRH has two sleep modes of operation with a minimum power consumption of 3.15 mW. Specific designs of heatsinks at CO for improving efficiency and MMF tapers for decreasing cost of the system are included.

The system functionalities tested include the sensing of different parameters of the RRH, and enabling different sleep modes. Finally, as a proof of concept, the system is used for feeding a RF-PA placed at the RRH providing a stable power supply and EVM performance below 17.8% with QPSK on a 20 GHz RF carrier.

Acknowledgment

The authors thank D. S. Montero for his work supporting the MMF optical power link design.

References

[1] C. Algora and R. Peña, "Recharging the battery of implantable biomedical devices by light," *Artif. Organs*, vol. 33, no. 10, pp. 855–860, 2009.
[2] R. Peña, C. Algora, I. R. Matías, and M. López-Amo, "Fiber-based 205-mW (27% efficiency) power-delivery system for an all-fiber network with optoelectronic sensor units," *Appl. Opt.*, vol. 38, no. 12, pp. 2463–2466, 1999.
[3] K. Worms *et al.*, "Reliable and lightning-safe monitoring of wind turbine rotor blades using optically powered sensors," *Wind Energ.*, vol. 20, no. 2, pp. 345–360, 2017.
[4] J. D. López-Cardona, D. S. Montero, and C. Vázquez, "Smart remote nodes fed by power over fiber in Internet of Things applications," *IEEE Sensors J.*, vol. 19, no. 17, pp. 7328–7334, Sep. 2019.
[5] B. Guzowski, R. Gozdur, and M. Lakomski, "WDM power supply for identification system of fibre optic connectors," *Metrol. Meas. Syst.*, vol. 25, no. 1, pp. 235–244, 2018.
[6] M. Roeger *et al.*, "In-service monitoring of PON access networks with powerline independent devices," *IEEE/OSA J. Opt. Commun. Netw.*, vol. 6, no. 11, pp. 1018–1027, Nov. 2014.
[7] M. Röger *et al.*, "Optically powered fiber networks," *Opt. Exp.*, vol. 16, no. 26, pp. 21821–21834, 2008.
[8] H. Miyakawa, Y. Tanaka, and T. Kurokawa, "Design approaches to power-over-optical local-area-network systems," *Appl. Opt.*, vol. 43, no. 6, pp. 1379–1389, 2004.
[9] R. S. Penze, J. B. Rosolem, U. Duarte, G. Paiva, and R. B. Filho, "Fiber powered extender for XG-PON/G-PON applications," *J. Opt. Commun. Netw.*, vol. 6, no. 3, pp. 250–258, 2014.
[10] G. Otero *et al.*, "SDN-based multi-core power-over-fiber (PoF) system for 5G fronthaul: Towards PoF pooling," in *Proc. 44th Eur. Conf. Opt. Commun.*, 2018, pp. 1–3.
[11] M. Matsuura and J. Sato, "Bidirectional radio-over-fiber systems using double-clad fibers for optically powered remote antenna units," *IEEE Photon. J.*, vol. 7, no. 1, Feb. 2015, Art. no. 7900609.
[12] T. Umezawa, P. T. Dat, K. Kashima, A. Kanno, N. Yamamoto, and T. Kawanishi, "100-GHz radio and power over fiber transmission through multicore fiber using optical-to-radio converter," *J. Lightw. Technol.*, vol. 36, no. 2, pp. 617–623, Jan. 2018.
[13] C. Vázquez *et al.*, "Integration of power over fiber on RoF systems in different scenarios," in *Proc. SPIE, Broadband Access Commun. Technol. XI*, Jan. 2017, Art. no. 101280E.
[14] C. Vázquez *et al.*, "Monitoring systems and remote powering for next generation broadband access networks," in *Proc. 19th Int. Conf. Transparent Opt. Netw.*, Jul. 2017, pp. 1–4.
[15] M. Matsuura and Y. Minamoto, "Optically powered and controlled beam steering system for radio-over-fiber networks," *J. Lightw. Technol.*, vol. 35, no. 4, pp. 979–988, Feb. 2017.
[16] I. Ashraf, F. Boccardi, and L. Ho, "Sleep mode techniques for small cell deployments," *IEEE Commun. Mag.*, vol. 49, no. 8, pp. 72–79, Aug. 2011.

[17] J. Wu, Y. Zhang, M. Zukerman, and E. K.-N. Yung, "Energy-efficient base-stations sleep-mode techniques in green cellular networks: A survey," *IEEE Commun. Surv. Tut.*, vol. 17, no. 2, pp. 803–826, Apr.–Jun. 2015.
[18] J. Liu, M. Sheng, L. Liu, and J. Li, "Network densification in 5G: From the short-range communications perspective," *IEEE Commun. Mag.*, vol. 55, no. 12, pp. 96–102, Dec. 2017.
[19] I. Tafur *et al.*, "Space division multiplexing 5G fronthaul with analog and digital radio-over-fiber and optical beamforming- the blueSPACE concept," pp. 1–15, Aug. 2018.
[20] A. P. Goutzoulis, J. M. Zomp, and A. H. Johnson, "Development and antenna range demonstration of an eight-element optically powered directly modulated receive UHF fiberoptic manifold," *J. Lightw. Technol.*, vol. 14, no. 11, pp. 2499–2505, Nov. 1996.
[21] C. Lethien *et al.*, "Energy-autonomous picocell remote antenna unit for radio-over-fiber system using the multiservices concept," *IEEE Photon. Technol. Lett.*, vol. 24, no. 8, pp. 649–651, Apr. 2012.
[22] M. Matsuura and J. Sato, "Bidirectional radio-over-fiber systems using double-clad fibers for optically powered remote antenna units," *IEEE Photon. J.*, vol. 7, no. 1, pp. 1–9, Feb. 2015.
[23] M. Matsuura, H. Nomoto, H. Mamiya, T. Higuchi, D. Maason, and S. Fafard, "Over 40-W electric power and optical data transmission using an optical fiber," *IEEE Trans. Power Electron.*, vol. 36, no. 4, pp. 4532–4539, Apr. 2021.
[24] C. Vázquez *et al.*, "Multicore fiber scenarios supporting power over fiber in radio over fiber systems," *IEEE Access*, vol. 7, pp. 158409–158418, Oct. 2019.
[25] Nokia, Esppo, Finland, "Nokia confirms 5G as 90 percent more energy efficient," Dec. 20, 2020. [Online]. Available: https://www.nokia.com/about-us/news/releases/2020/12/02/nokia-confirms-5g-as-90-percent-more-energy-efficient/
[26] S. Rommel *et al.*, "Towards a scaleable 5G fronthaul: Analog radio-over-fiber and space division multiplexing," *J. Lightw. Technol.*, vol. 38, no. 19, pp. 5412–5422, Oct. 2020.
[27] J. D. López-Cardona, C. Vázquez, D. S. Montero, and P. C. Lallana, "Remote optical powering using fiber optics in hazardous environments," *J. Lightw. Technol.*, vol. 36, no. 3, pp. 748–754, Feb. 2018.
[28] C. Vázquez, D. S. Montero, F. M. A. Al-Zubaidi, and J. D. López-Cardona, "Experiments on shared and dedicated power over fiber scenarios in multicore fibers," in *Proc. 28th Eur. Conf. Netw. Commun.*, 2019, pp. 412–415.
[29] H. Helmers, C. Armbruster, M. von Ravenstein, D. Derix, and C. Schöner, "6-W optical power link with integrated optical data transmission," *IEEE Trans. Power Electron.*, vol. 35, no. 8, pp. 7904–7909, Aug. 2020.

Juan Dayron López Cardona received the M.Sc. degree in electronics systems engineering from Universidad Carlos III of Madrid, Madrid, Spain, in 2016, where he is currently working toward the Ph.D. degree. His research interests include low power electronics, multicore optical fibers, and power over fiber systems.

Pedro Contreras Lallana received the Ph.D. degree from Universidad Carlos III of Madrid (UC3M), Madrid, Spain, in 2011. He is currently a Visiting Associate Professor with Electronics Technology Department, UC3M. His current research interests include fiber-optic sensors, integrated optics, switches, and power over fiber systems.

Rubén Altuna received the M.Sc. degree in electronics systems engineering from Universidad Carlos III of Madrid, Madrid, Spain, in 2020. His research interests include radio over fiber, instrumentation systems, and power over fiber systems.

Alicia Fresno-Hernández received the M.Sc. degree in photonics engineering from Universidad Carlos III of Madrid, Madrid, Spain, in 2020. Her research interests include optical fiber tapers, power over fiber applications, optical forces, and nanophotonics.

Xabier Barreiro currently working toward the M.Sc. degree in industrial engineering from UNED - Universidad Nacional de Educación a Distancia, Madrid, Spain. His research interests include optical fiber pyrometry, thermal designs, and power over fiber applications.

Carmen Vázquez (Senior Member, IEEE) is currently a Full Professor with Electronics Technology Department, Universidad Carlos III of Madrid, Madrid, Spain. She was with TELECOM, Denmark, and Telefónica Investigación y Desarrollo, Spain. She was a Visiting Scientist with RLE Massachusetts Institute of Technology, Cambridge, MA, USA. Her research interests include integrated optics, optical communications, instrumentation with plastic and multicore optical fibers, fiber optic sensors, Power over Fiber, and WDM-PON networks. She is also a Fellow of SPIE.